

Strengths of Rock Fractures as Affected by Shear Velocities and Confinements

Kleempmek M.* and FuenkajornK.

*Geomechanics Research Unit, Suranaree University of Technology
111 University Avenue, NakhonRatchasima 30000, Thailand
matseekleempmek@gmail.com*

Abstract

The objective of this study is to experimentally investigate the rate-dependent shear strength of rock fractures by performing triaxial shear testing under various shear velocities and confinements. A polyaxial load frame is used to perform the shear tests on tension-induced fractures prepared in $50 \times 50 \times 87$ mm³ rectangular blocks. The fracture area is 50×10 mm². The specimens are prepared from granite, marl and sandstone. The confining pressures vary from 1, 3, 7, 12 to 18 MPa. The axial stresses are applied under constant rates equivalent to the shear velocities on the fractures from 8.7×10^{-6} to 8.7×10^{-3} mm/s. The asperity amplitudes on the fracture planes are measured from laser-scanned profiles along the shear direction and used to estimate the joint roughness coefficients (JRC) of the fracture. The JRC's are averaged as 15, 8 and 6 for the granite, marl and sandstone. The test results indicate that the peak shear strengths under each confinement increases with shear velocities. The Barton's criterion is modified here to explicitly incorporate the shear velocity and confining pressure. The peak shear strength (τ) is presented as:

$$\tau = \sigma_n \cdot \tan \{ \phi_b^* + JRC \cdot \log [\kappa \cdot (d_s)^\lambda \cdot \exp(\beta \cdot \sigma_3) / \sigma_n] \}$$
 where σ_n = normal stress, ϕ_b^* = basic friction angle or apparent friction angle of saw cut surface, κ , λ , and β are empirical constants, d_s = shear velocity, and σ_3 = confining pressure. The equation fits well to the experimental results for all rock types. It allows a transition to the conventional direct shear test results by setting σ_3 equal to zero. The equation can be used to predict rock fracture shear strengths under confining pressures and shear velocities beyond those used in this study.

Keywords: Joint, Shear strength, Triaxial shear test, Confinement, Shear velocity.

1. Introduction

Understanding the nature behavior of rock mass is important in many geotechnical applications. The performance of engineering structures constructed in rock is concerned with the presence of fractures in rock when subjected to forces and displacements (Curran and Leong, 1983; Li et al., 2012). In rock masses, properties such as roughness, separation and joint aperture have considerable effects on shear strength of rock fractures. The shear behavior of rock fractures is usually estimated through direct shear tests (e.g., ASTM D5607-08) to determine the peak and residual strengths of the rock fractures. Its test configurations however pose some disadvantages that the magnitudes of the applied normal stress are limited by the uniaxial compressive strength of the rock and that the fractures are sheared under unconfined conditions. The triaxial shear testing (Brady and Brown, 2006; Jaeger et al., 2007) has been developed to simulate the frictional resistance of rock fractures under confinements. The normal stress at which the shear strengths are measured can be controlled by the applied axial stress and confining pressure.

The effect of shear velocity on rock fractures shear strength plays an important role in the stability and safety assessment of the underground structures subjected to loading. Rapid loading or high shear velocity (seismic load and blasting) may impose different behavior to the shearing resistance of rock fractures, as compound to the slow loading or low velocity of displacement (Crawford and Curran, 1981; Li et al., 2012; Chokchai, 2013). The shear velocity can also affect the shearing resistance of rock fractures, quantitative assessment of such effect has been rare.

The objective of this study is to determine the effects of shear velocity on fracture shear strength of rocks under confinement. The effort involves performing triaxial shear tests on tension-induced fractures and smooth saw-cut surfaces by using a polyaxial load frame. Mathematical relationships between the shear velocity and the fractures shear strength are proposed to predict the shear strengths subject under various loading rates and confinements.

2. Samples preparation

The rock samples used in this study are Tak granite (Mahawat et al., 1990), Lopburi marl (Bunopas, 1992) and PhraWihan sandstone (BoonsenerandSonpiron, 1997) which have been prepared to obtain rectangular block specimens with nominal dimensions of $50 \times 50 \times 87 \text{ mm}^3$ and fracture surface with an area of $50 \times 87 \text{ mm}^2$. The fractures are artificially made in the laboratory by tension inducing method. The normal to the fracture plane makes an angle 60° with the axis of the specimens. All fractures are clean and well mated. The asperity amplitudes on the fracture planes are measured from the laser-scanned profiles along the shear direction. The readings are made to the nearest 0.01 mm. Fig. 1 shows laser scanned images of a tension-induced fracture and the directions of the applied stresses with respect to the fracture orientation. The maximum amplitudes are used to estimate the joint roughness coefficients (JRC) of each fracture based on Barton’s chart (Barton, 1982). The joint roughness coefficients are averaged as 15, 8 and 6 for the Tak granite, Lopburi marl and PhraWihan sandstone, respectively.

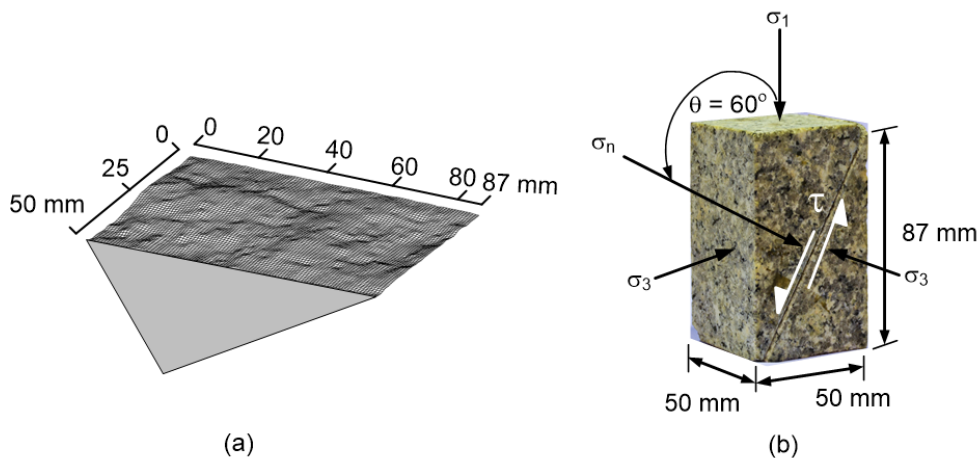


Fig. 1. Laser scanned images of fracture in granite (a) and the directions of applied stresses with respect to the fracture orientation (b).

3. Triaxial shear test

The rock is installed into the polyaxial load frame (Fig.2) (FuenkajornandKenkhunthod, 2010). Neoprene sheets are used to minimize the friction at all interfaces between the loading platen and the rock surface. A polyaxial load frame is applying the constant confining pressures (σ_3) from 1, 3, 7, 12 to 18 MPa. The specimen is first under hydrostatic condition. The axial stress is applied at a constant rate varying from 10^{-5} to 10^{-2} mm/s . Digital pressure gages measure oil pressure in the hydraulic cylinders that applies the axial stresses to the rectangular specimens. The peak shear strength is recorded. The test is terminated when a total shear displacement of 8 mm is reached. After shearing the fractures are examined and photographed.

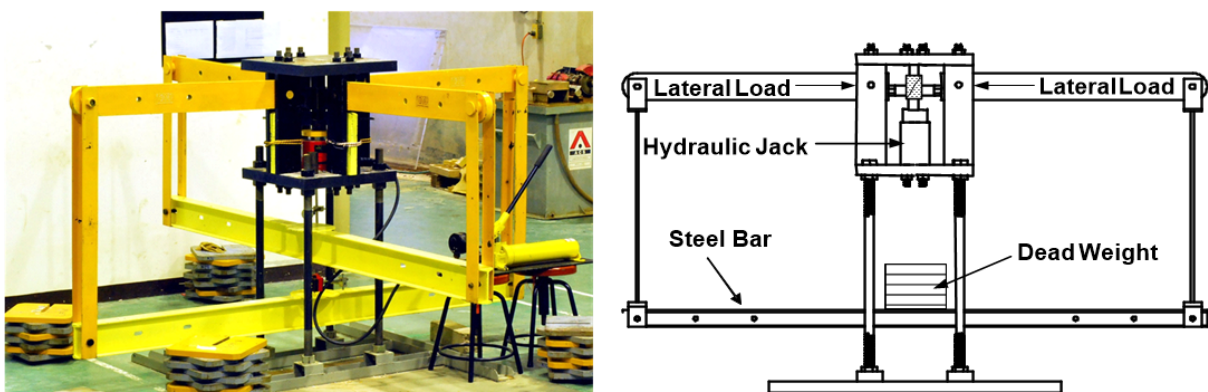


Fig. 2. Polyaxial load frame and the directions of applied stress on the fracture plane (FuenkajornandKenkhunthod, 2010).

The shear stress (τ) and its corresponding normal stress (σ_n) can be determined from the applied principal stresses (σ_1 and σ_3) as follows:

$$\tau = \frac{1}{2}(\sigma_1 - \sigma_3) \cdot \sin 2\beta \tag{1}$$

$$\sigma_n = \frac{1}{2}(\sigma_1 + \sigma_3) + \frac{1}{2}(\sigma_1 - \sigma_3) \cdot \cos 2\beta \tag{2}$$

The shear displacements can be calculated as:

$$d_s = \frac{1}{2}(d_1 - d_3) \cdot \sin 2\beta \tag{3}$$

where β is the angle between σ_1 and σ_n directions. For all specimens the angle β equals to 60 degrees. d_1 and d_3 are the fracture displacements monitored in the axial direction and the direction normal to the strike of the fracture during the test, respectively. From Eq. (3) the rate shear displacements (\dot{d}_s) that are equivalent to \dot{d}_1 from 10^{-5} to 10^{-2} mm/s can be determined as 8.7×10^{-6} to 8.7×10^{-3} mm/s.

4. Test results

Table 1 summarizes the shear strength results for the three rock types. The shear stresses-displacements (τ - d_s) curves for the three rock types are shown in Figs. 3 through 5. It is clear that the shear strength at each confinement increases with the shear velocities.

Table 1. Summary of peak shear strengths and their corresponding normal stresses.

\dot{d}_s (mm/s)	σ_3 (MPa)	Granite			Sandstone			Marl		
		σ_1 (MPa)	σ_n (MPa)	τ (MPa)	σ_1 (MPa)	σ_n (MPa)	τ (MPa)	σ_1 (MPa)	σ_n (MPa)	τ (MPa)
8.7×10^{-3}	1	82.32	21.33	35.21	40.32	10.83	17.03	42.00	11.25	17.75
	3	97.44	26.61	40.89	65.32	18.58	26.98	58.80	16.95	24.16
	7	117.60	34.65	47.89	89.04	27.51	35.52	84.00	26.25	33.34
	12	142.80	44.70	56.64	114.24	37.56	44.27	110.88	36.72	42.82
	18	168.00	55.50	64.95	139.44	48.36	52.59	134.40	47.10	50.40
8.7×10^{-4}	1	65.52	17.13	27.94	35.28	9.57	14.84	35.28	9.57	14.84
	3	78.96	21.99	32.89	58.23	16.81	23.91	52.08	15.27	21.25
	7	97.44	29.61	39.16	80.64	25.41	31.89	75.60	24.15	29.70
	12	120.96	39.24	47.18	106.41	35.60	40.88	97.44	33.36	37.00
	18	144.48	49.62	54.77	129.23	45.81	48.16	121.23	43.81	44.70
8.7×10^{-5}	1	47.04	12.51	19.94	28.56	7.89	11.98	28.90	7.97	12.08
	3	60.48	17.37	24.89	50.40	14.85	20.52	44.39	13.35	17.92
	7	80.64	25.41	31.89	72.24	23.31	28.25	65.86	21.71	25.49
	12	102.48	34.62	39.18	97.74	33.44	37.13	85.68	30.42	31.90
	18	124.32	44.58	46.04	120.02	43.50	44.18	107.52	40.38	38.76
8.7×10^{-6}	1	33.94	8.48	12.95	23.52	6.63	9.75	21.84	6.21	9.02
	3	45.36	13.59	18.34	42.67	12.92	17.18	37.03	11.51	14.73
	7	64.01	21.25	24.69	63.84	21.21	24.61	58.80	19.95	22.43
	12	82.32	29.58	30.45	87.73	30.93	32.79	76.27	28.07	27.83
	18	104.16	39.54	37.31	109.20	40.80	39.49	94.08	37.02	32.94

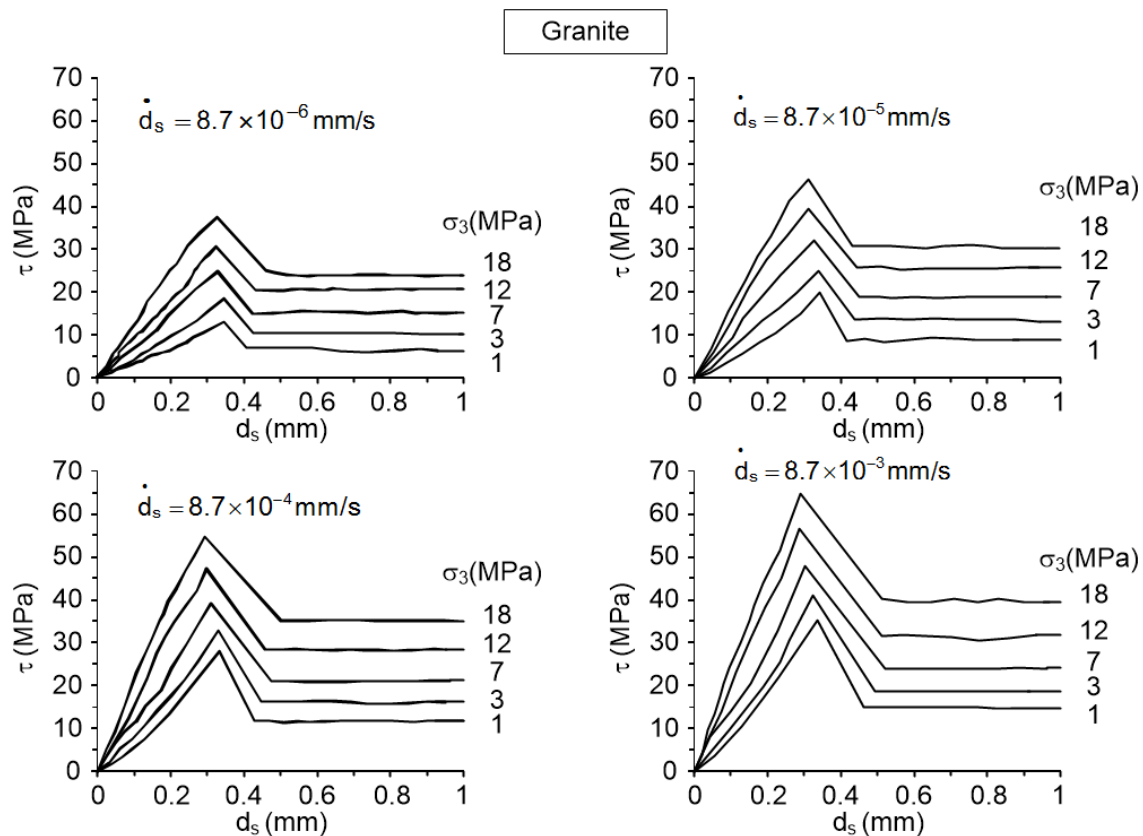


Fig. 3. Shear stresses (τ) as a function of shear displacement (d_s) for granite.

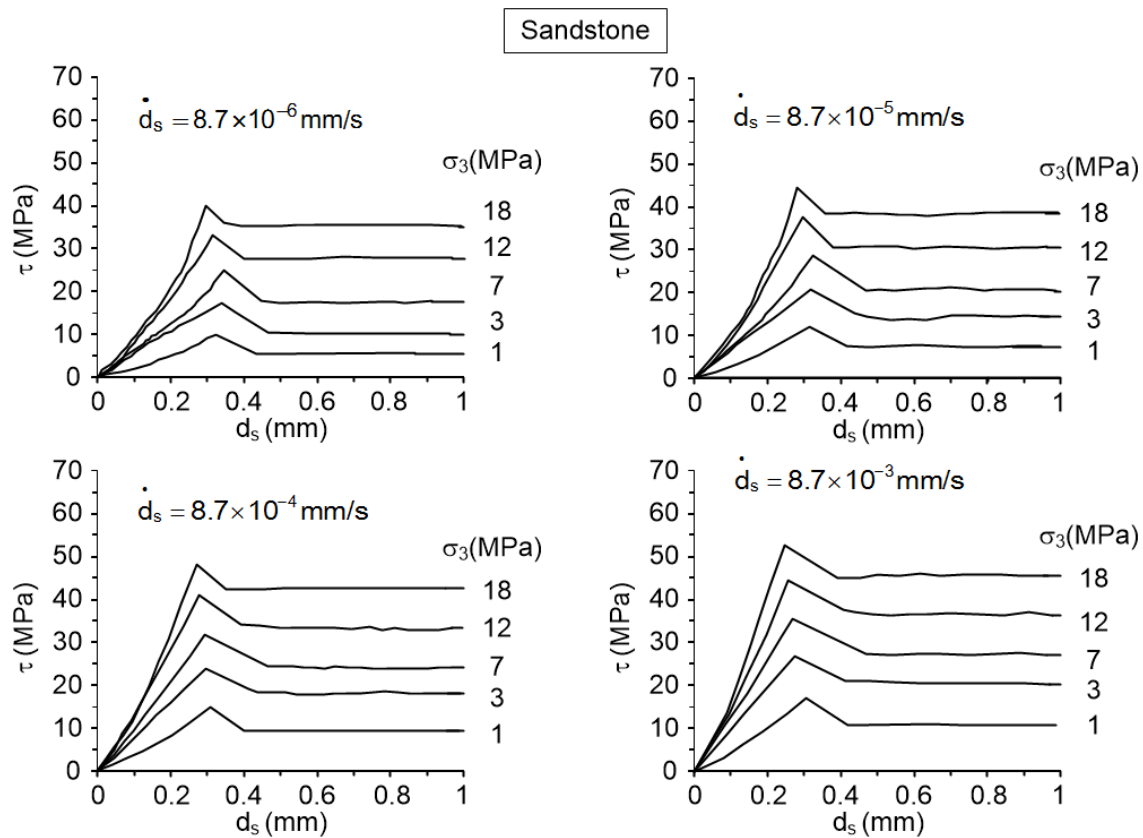


Fig. 4. Shear stresses (τ) as a function of shear displacement (d_s) for sandstone.

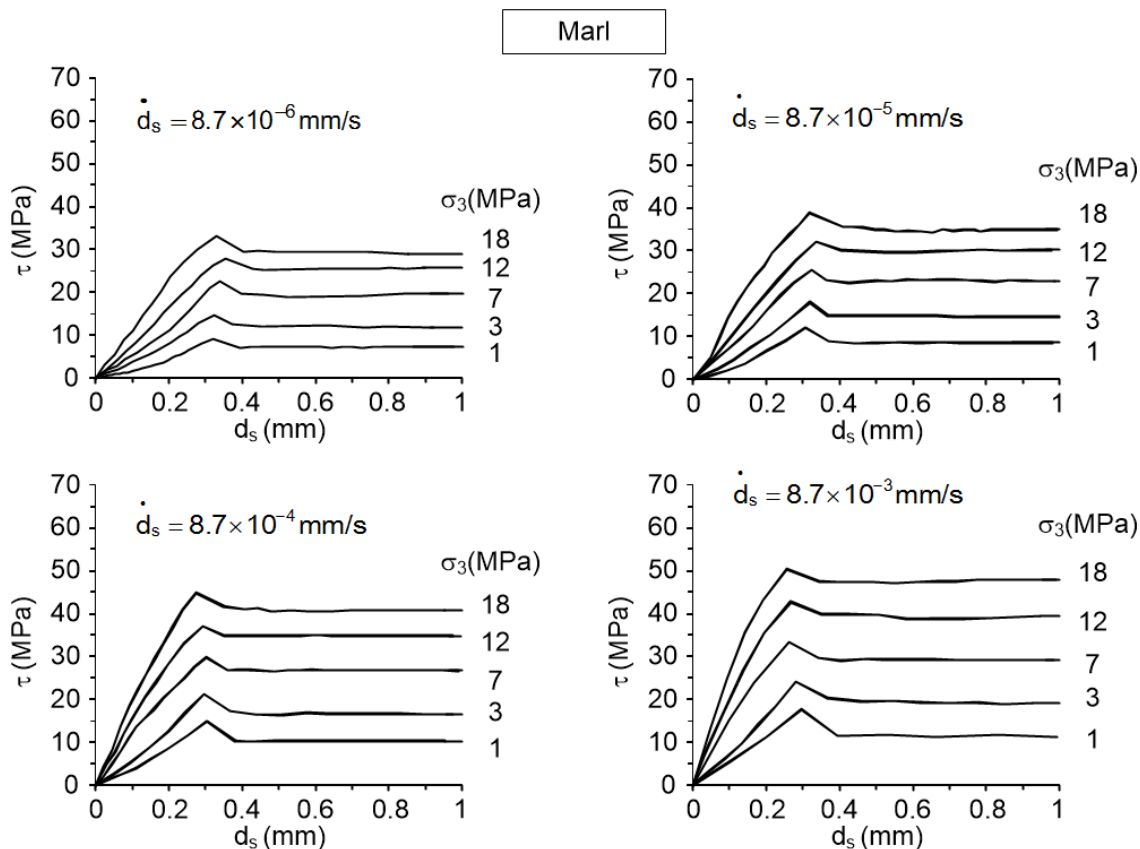


Fig. 5. Shear stresses (τ) as a function of shear displacement (d_s) for marl.

Post-test observation on the sheared off areas indicates that the asperity areas that have been sheared off under each confinement increases with the shear velocities. Some post-test fractures in the marl specimens are shown in Fig. 6.

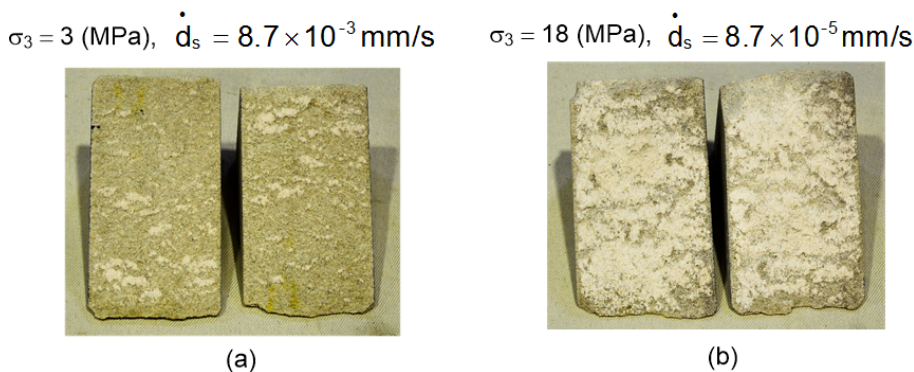


Fig. 6. Some post-test fracture of marl: (a) confinement = 3 MPa and shear velocities = 8.7×10^{-3} and (b) confinement = 18 MPa and shear velocities = 8.7×10^{-5} .

5. Triaxial shear test of smooth saw-cut surfaces.

Shear strengths of saw-cut surfaces are determined to assess the effects of shear velocities and confinements on the shearing resistance of smooth surfaces. The test method and strength calculation are identical to those of the tension-induced fractures. The confining pressures are 1, 7, and 12 to MPa. The shear velocities on the fractures are 8.7×10^{-3} and 8.7×10^{-6} mm/s. The Coulomb's criterion is used to represent the peak shear strengths under various shear velocities and confinements:

$$\tau = \sigma_n \cdot \tan(\phi^*) + c^* \tag{4}$$

where ϕ^* and c^* are defined here as the apparent friction angle and apparent cohesion of the saw-cut surfaces. This is primarily to avoid confusing with the fracture cohesion (c) and friction angle (ϕ) conventionally obtained from the direct shear test with constant normal stress. The above equation is fitted to the experimental results in the forms of τ - σ_n diagrams in Fig. 7. The shearing resistances for the smooth surfaces of the three rock types tend to be independent of the shear velocities \dot{d}_s , as evidenced by the similar values of ϕ^* and c^* obtained from different shear velocities.

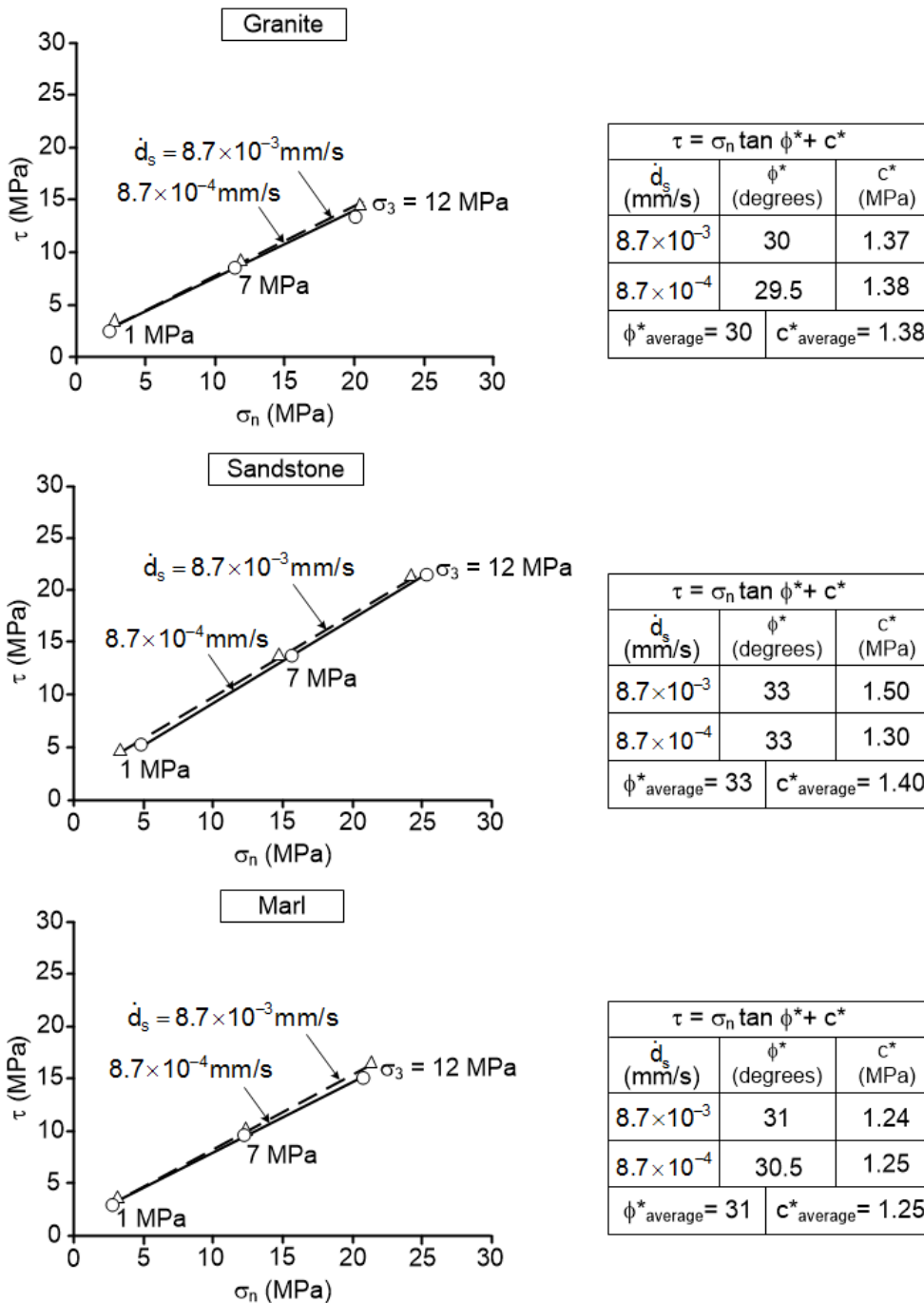


Fig. 7. Shear strength of smooth saw-cut surfaces.

6. Barton strength criterion

The Barton's criterion is proposed here to represent the peak shear strengths of tension-induced fractures:

$$\tau = \sigma_n \cdot \tan(\phi_b^* + JRC \cdot \log(\sigma_j^*/\sigma_n)) \tag{5}$$

where ϕ_b^* represents the basic friction angle or apparent friction angle of saw cuts surface, σ_j^* is apparent joint wall compressive strength under confinements at each shear velocity, Regression analysis performed to determine σ_j^* in Eq. (5). The basic friction angle shown in Fig. 7. The results of the regression analysis are shown in Table 2.

Table 2. Apparent joint wall strengths obtained from applying Barton criterion.

\dot{d}_s (mm/s)	σ_3 (MPa)	σ_j^* (MPa)		
		Granite	Sandstone	Marl
8.7×10^{-3}	1	2,410	287,077	667,169
	3	2,264	220,958	358,222
	7	1,908	95,602	164,789
	12	1,704	48,919	91,638
	18	1,502	26,138	46,028
8.7×10^{-4}	1	1,846	200,878	477,681
	3	1,677	161,782	251,705
	7	1,355	65,052	107,410
	12	1,194	34,898	48,199
	18	1,040	17,124	25,379
8.7×10^{-5}	1	1,230	141,903	313,786
	3	1,111	105,684	151,069
	7	930	41,018	58,185
	12	810	22,736	23,835
	18	698	11,090	11,962
8.7×10^{-6}	1	704	89,720	159,963
	3	677	61,293	78,746
	7	557	23,315	33,481
	12	457	12,657	11,866
	18	416	6,142	4,779

The results clearly indicate that σ_j^* decreases as σ_3 increase. An empirical equation is proposed to predict the σ_j^* as a function of σ_3 :

$$\sigma_j^* = \alpha \cdot \exp(-\beta \cdot \sigma_3) \quad (6)$$

where α and β are empirical constants. For the three rock types these empirical constants are defined by the regression analysis as shown in Table 3. Good correlation is obtained ($R^2 > 0.9$). The decrease of empirical constants, α with shear velocities, \dot{d}_s can be best described by a power equation (Fig. 8):

$$\alpha = \kappa \cdot (\dot{d}_s)^\lambda$$

where κ and λ are empirical constants from each rock as shown in Table 4.

Substituting Eq. (7) into (6) the apparent joint wall compressive strength can be presented as a function of shear velocities and confinements:

$$\sigma_j^* = \kappa \cdot (\dot{d}_s)^\lambda \cdot \exp(\beta \cdot \sigma_3) \quad (8)$$

Table 3. Constants α and β for each rock.

\dot{d}_s (mm/s)	α			β		
	Granite	Sandstone	Marl	Granite	Sandstone	Marl
8.7×10^{-3}	32	4,800	15,500	0.03	0.15	0.19
8.7×10^{-4}	24	3,550	11,100	0.03	0.15	0.19
8.7×10^{-5}	16	2,500	7,000	0.03	0.15	0.19
8.7×10^{-6}	10	1,400	3,000	0.03	0.15	0.19

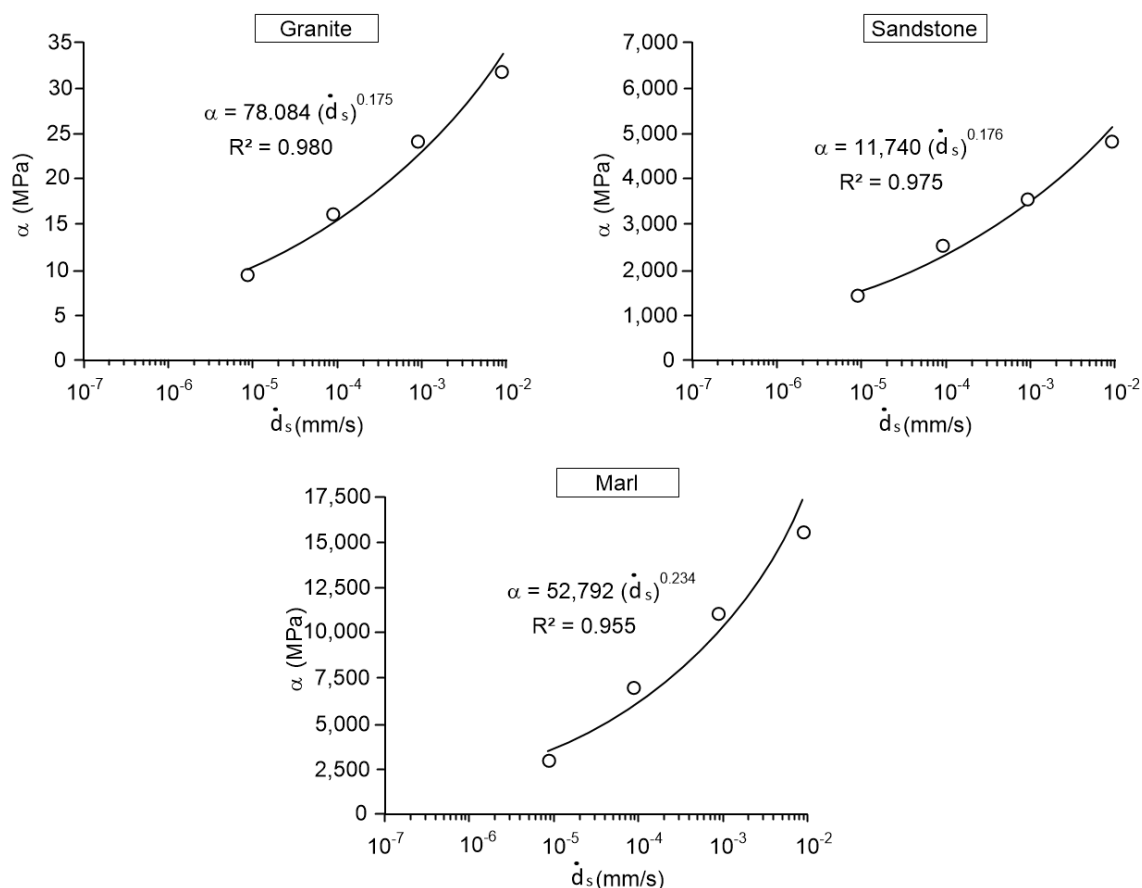


Fig. 8. Empirical constants, α as a function of shear velocity (\dot{d}_s) for all rock types.

Table 4 Constants κ , λ and β for each rock.

Rock Types	$\sigma_j^* = \kappa \cdot (\dot{d}_s)^\lambda \cdot \exp(\beta \cdot \sigma_3)$		
	κ	λ	β
Granite	78.084	0.175	0.03
Sandstone	11,740	0.176	0.15
Marl	52,792	0.234	0.19

Substituting Eq. (8) into (5) the complete for the shear strength criterion is obtained:

$$\tau = \sigma_n \cdot \tan \{ \phi_b^* + JRC \cdot \log [\kappa \cdot (\dot{d}_s)^\lambda \cdot \exp(-\beta \cdot \sigma_3) / \sigma_n] \} \quad (9)$$

The modified Barton's criterion agrees reasonably well with the test results as shown in Fig.9. The figures are shown the upper and lower bounds of the peak shear strength obtained from the triaxial shear tests method. The upper bound is define by the angle between the normal of fracture and the axial direction which is maintain constant at 60 degrees. The lower bound is define as on basic friction angle from smooth saw-cut surfaces test method.

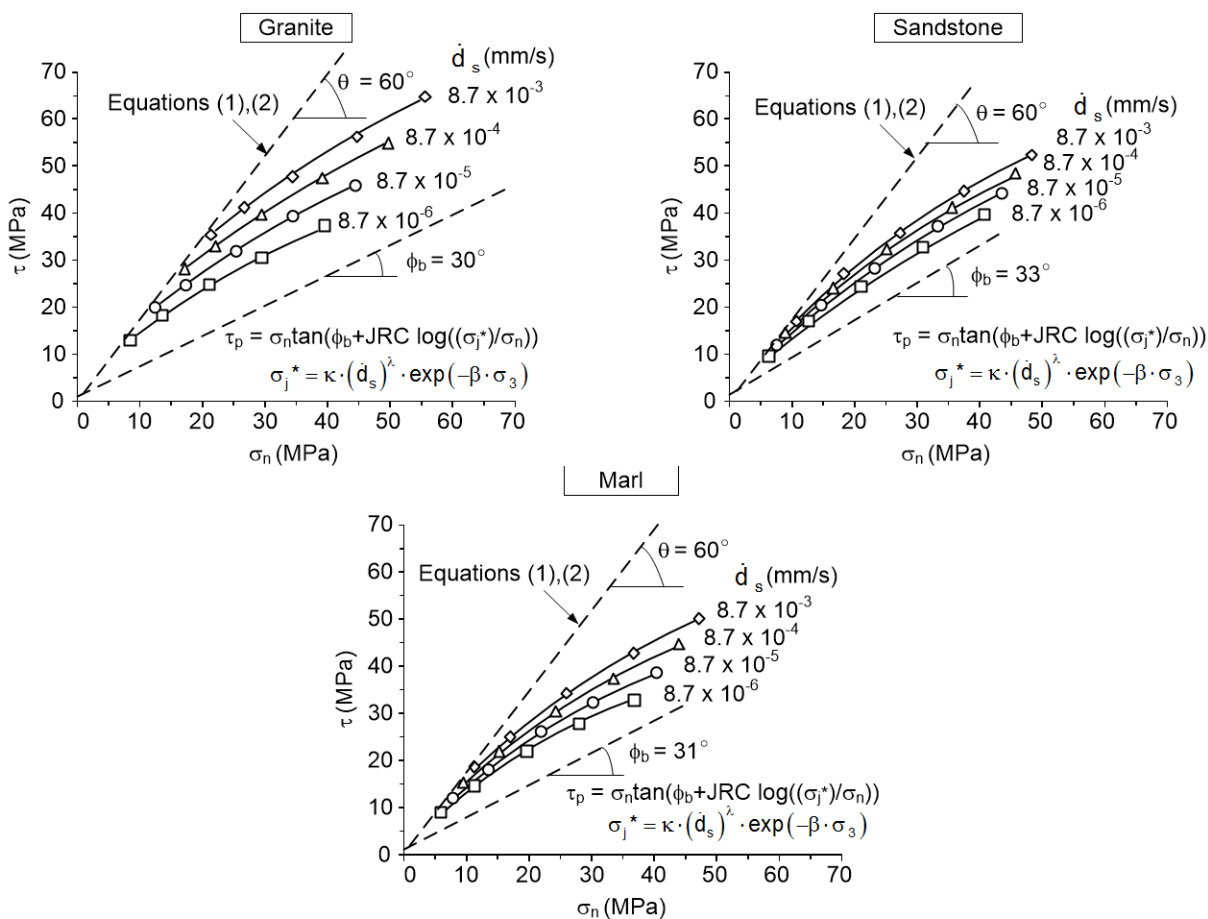


Fig. 9. Peak shear strengths from the modified Barton's criterion.

7. Discussions and conclusions

The results imply that the shear velocity dependency of rough fracture is primarily due to the time-dependent strength of the rock asperities on the fracture wall. This supported by the experimental results obtained by Fuenkajorn & Khenkhunthod (2010) who conclude that the uniaxial and triaxial compressive strengths and elastic modulus of rocks increase exponentially with the loading rate. It can therefore be postulated that the time-dependent shear strengths of the fractures may be found in other rock types of which compressive strengths are sensitive to loading rate.

In general the increase of the shear stresses and the normal stress with confining pressures as observed here agrees reasonably well with the results obtained by Kapang et al. (2013). The confining pressures decrease the apparent joint wall compressive strengths. The decrease can be described by an exponential equation (Eq. 8). This means that the fracture shear strengths from the (unconfined) direct shear testing may not truly represent the fault or fracture shear strengths under the confinements of in-situ conditions.

The shearing resistances for the smooth surfaces of the three rock types tend to be independent of the shear velocity. It may be postulated that the effects of the shear velocity may relate to the fracture roughness, asperity amplitude and strength of the rock walls (hardness of rock surface).

The effect of shear velocity tends to pronounce more on the strong rocks with rough fracture surfaces (granite) as compared to the softer rocks with relatively smooth fracture surfaces (marl).

The fractures tested here are quite similar for joint roughness coefficients (JRC = 6-15) and small fracture area (50×87 mm²), and obtained from only three rock types. More testing is desirable on

various rock types and fracture characteristics to further investigate the effects of fracture roughness, scale (e.g. Fardin et al., 2001), and strength of the asperities (e.g. Yang et al., 2001), and incorporate them into the proposed shear strength criterion.

Acknowledgements

This study is funded by Suranaree University of Technology and by the Higher Education Promotion and National Research University of Thailand. Per-mission to publish this paper is gratefully acknowledged.

References

- ASTM D5607-08, Standard test method for performing laboratory direct shear strength tests of rock specimens under constant normal force, *Annual Book of ASTM Standards*, Vol. 04.08. West Conshohocken, PA: American Society for Testing and Materials.
- Barton, N., 1982, Characterizing rock masses to improve excavation design. Panel Report, Theme II Tunnelling and Excavation, *Proc. of 4th Congress IAEG*, New Delhi.
- Boonsener, M. and Sonpiron, K., 1997, Correlation of tertiary rocks in northeast, Thailand, *Proc. of International Conference on Stratigraphy and Tectonic Evolution of Southeast Asia and the South Pacific*, Bangkok, Thailand. 19-24 August.
- Brady, B.H.G. and Brown, E.T., 2006, *Rock Mechanics for Underground Mining* (3rd. Edn.), Springer, Netherlands.
- Bunopas, S., 1992, *Regional stratigraphic correlation in Thailand. National Conference on Geological Resources of Thailand: Potential for Future Development*, Department of mineral Resources. Bangkok, Thailand, 17-24 November 1992.
- Chokchai, B. and Fuenkajorn, K., 2013, Effects of loading rate on joint shear strength in sandstones, *Proc. of Fourth Thailand Symposium on Rock Mechanics*, NakhonRatchasima, Thailand, 297-308.
- Crawford, A.M. and Curren, J.H., 1981, The influence of shear velocity on the frictional resistance of rock discontinuities, *Int. J. Rock Mech. Min. Sci. Geomech. Abstr.*, 18, 505-515.
- Curran, J.H. and Leoung, P.K., 1983, Influence of shear velocity on rock joint strength, *Proc. of International Congress on Rock Mechanics*, 5, Melbourne, A235-A240.
- Fardin, N., Stephansson, O. and Jing, L., 2001, The scale dependence of rock joint surface roughness, *Int. J. Rock Mech. Min. Sci.*, 38, 659-669.
- Fuenkajorn, K. and Kenkhunthod, N., 2010, Influence of loading rate on deformability and compressive strength of three Thai sandstones, *Geotech. Geol. Eng.*, 28, 707-715.
- Jaeger, J.C., Cook, N.G.W. and Zimmerman, R.W., 2007, *Fundamentals of Rock Mechanics* (4th. Edn.). Blackwell Publishing, Malden.
- Kapang, P., Walsri, C., Sriapai, T. and Fuenkajorn, K., 2013, Shear strengths of sandstone fractures under true triaxial stresses, *J. Struct. Geol.*, 48, 57-7.
- Li, B., Jing, Y. and Wang, G., 2012, Evaluation of shear velocity dependency of rock fractures by using repeated shear tests, *Proc. of 12th ISRM Congress, Harmonising Rock Engineering and the Environment*, 16-21 October, Beijing, China, 699-702.
- Mahawat, C., Atherton, M.P. and Brotherton, M.S., 1990, The Tak Batholith, Thailand: the evolution of contrasting granite types and implications for tectonic setting, *J. Southeast Asian Earth Sci.*, 4, 11-27.
- Yang, Z.Y., Di, C.C. and Yen, K.C., 2001, The effect of asperity order on the roughness of rock joints, *Int. J. Rock Mech. Min. Sci.*, 38, 745-752.